

Radiation Effects in Quantum Well Detectors

Omar Manasreh

October 2001

Final Report

APPROVED FOR PUBLIC RELEASE; DISTRIBUTION IS UNLIMITED.

20020213 128



**AIR FORCE RESEARCH LABORATORY
Space Vehicles Directorate
3550 Aberdeen Ave SE
AIR FORCE MATERIEL COMMAND
KIRTLAND AIR FORCE BASE, NM 87117-5776**

AFRL-VS-TR-2001-1112

Using Government drawings, specifications, or other data included in this document for any purpose other than Government procurement does not in any way obligate the U.S. Government. The fact that the Government formulated or supplied the drawings, specifications, or other data, does not license the holder or any other person or corporation; or convey any rights or permission to manufacture, use, or sell any patented invention that may relate to them.

This report has been reviewed by the Public Affairs Office and is releasable to the National Technical Information Service (NTIS). At NTIS, it will be available to the general public, including foreign nationals.

If you change your address, wish to be removed from this mailing list, or your organization no longer employs the addressee, please notify AFRL/VSSS, 3550 Aberdeen Ave SE, Kirtland AFB, NM 87117-5776.


Do not return copies of this report unless contractual obligations or notice on a specific document requires its return.

This report has been approved for publication.



VAIDYA NATHAN, DR-III
Project Manager

FOR THE COMMANDER



KIRT S. MOSER, DR-IV
Chief, Spacecraft Technology Division

REPORT DOCUMENTATION PAGE

Form Approved
OMB No. 0704-0188

Public reporting burden for this collection of information is estimated to average 1 hour per response, including the time for reviewing instructions, searching existing data sources, gathering and maintaining the data needed, and completing and reviewing this collection of information. Send comments regarding this burden estimate or any other aspect of this collection of information, including suggestions for reducing this burden to Department of Defense, Washington Headquarters Services, Directorate for Information Operations and Reports (0704-0188), 1215 Jefferson Davis Highway, Suite 1204, Arlington, VA 22202-4302. Respondents should be aware that notwithstanding any other provision of law, no person shall be subject to any penalty for failing to comply with a collection of information if it does not display a currently valid OMB control number. PLEASE DO NOT RETURN YOUR FORM TO THE ABOVE ADDRESS.

1. REPORT DATE 5-10-2001		2. REPORT TYPE Final		3. DATES COVERED 1 Oct 1997 - 30 Sep 1999	
4. TITLE AND SUBTITLE Radiation Effects in Quantum Well Detectors				5a. CONTRACT NUMBER	
				5b. GRANT NUMBER	
				5c. PROGRAM ELEMENT NUMBER 61102F	
6. AUTHOR(S) Omar Manasreh				5d. PROJECT NUMBER 2305	
				5e. TASK NUMBER TJ	
				5f. WORK UNIT NUMBER 03	
7. PERFORMING ORGANIZATION NAME(S) AND ADDRESS(ES) AFRL/VSSS, 3550 Aberdeen Avenue Kirtland AFB, NM 87117				8. PERFORMING ORGANIZATION REPORT NUMBER AFRL-VS-TR-2001-1112	
9. SPONSORING / MONITORING AGENCY NAME(S) AND ADDRESS(ES) AFRL/AFOSR 801 North Randolph Street Arlington, VA 22203				10. SPONSOR/MONITOR'S ACRONYM(S)	
				11. SPONSOR/MONITOR'S REPORT NUMBER(S)	
12. DISTRIBUTION / AVAILABILITY STATEMENT Approved for public release; Distribution is unlimited.					
13. SUPPLEMENTARY NOTES					
14. ABSTRACT We performed photoluminescence (PL) measurements of interband transitions in InGaAs/AlGaAs multiple quantum wells before and after fast neutron irradiation. It is shown that the intensity of the intersubband transitions is dramatically decreased in heavily irradiated samples, which can be explained in terms of trapping of the two-dimensional electrons by the irradiation induced defects. A negative persistent effect was also observed in the heavily irradiated samples. It is noted that the recovery of the electrons from this effect occurs at two temperature stages with thresholds at ~140K and ~250K, which indicates that the electrons were released from two different traps as the temperature is increased. We also investigated the effects of 1 MeV proton beam with doses ranging between 1.0×10^{12} and 5.0×10^{14} cm ⁻² on GaAs/AlGaAs. It is observed that the total integrated area of the intersubband transitions are dramatically decreased as the irradiation dose is increased. This reduction was interpreted as being due to the trapping of the two-dimensional electron gas by the irradiation-induced-defects. The total integrated areas of the intersubband transitions were studied as a function of irradiation doses for samples cut from wafers with structures containing either bulk or superlattice barriers. The results reveal that the intersubband transitions in samples with superlattice barriers degrade at a faster rate as compared to those transitions in samples with bulk barriers.					
15. SUBJECT TERMS Quantum Well,neutron,electron,proton,irradiation,photoluminescence					
16. SECURITY CLASSIFICATION OF:			17. LIMITATION OF ABSTRACT unlimited	18. NUMBER OF PAGES 24	19a. NAME OF RESPONSIBLE PERSON Vaidya Nathan
a. REPORT unclassified	b. ABSTRACT unclassified	c. THIS PAGE unclassified			19b. TELEPHONE NUMBER (include area code) 505-846-4497

Standard Form 298 (Rev. 8-98)
Prescribed by ANSI Std. Z39.18

TABLE OF CONTENTS

LIST OF FIGURES	iv
LIST OF TABLES	vi
1.0 Neutron Irradiation effects in $\text{In}_{0.07}\text{Ga}_{0.93}\text{As}/\text{Al}_{0.4}\text{Ga}_{0.6}\text{As}$ Multiple Quantum Wells	1
2.0 Electron Irradiation Effects in $\text{InGaAs}/\text{AlGaAs}$ Multiple Quantum Wells	5
3.0 Proton Irradiation Effects in $\text{GaAs}/\text{AlGaAs}$ Multiple Quantum Wells	10
4.0 Conclusions	15
DISTRIBUTION LIST	16

LIST OF FIGURES

Figure	Page
1. Photoluminescence spectra obtained at $T = 25K$ and plotted as a function of fast neutron irradiation dose. Spectrum (a) was obtained for the reference sample (unirradiated). The rest of the spectra were obtained for samples irradiated with different doses as indicated.	2
2. Normalized integrated area (I/I_0) of the PL spectra plotted as a function of the fast neutron irradiation dose. I_0 is the integrated area of spectrum (a) and I is the integrated area for spectra (b) - (e) in Fig. 1.	3
3. The peak position energy of the spectra reported in Fig. 1 plotted as a function of the fast neutron irradiation dose.	4
4. Optical absorption spectra of intersubband transitions in InGaAs/AlGaAs multiple quantum wells at 295K and 77K. Spectra (a) and (b) were obtained for a reference sample (unirradiated) and spectra (c) and (d) were obtained for a sample irradiated with 2 MeV electron beam and a dose of $5 \times 10^{17} \text{ cm}^{-2}$.	7
5. The total integrated area of the intersubband transition between the ground and first excited states in the electron irradiated InGaAs/AlGaAs multiple quantum wells measured as a function of temperature. The vertical arrows indicate the threshold temperatures at which the electrons are released from the irradiation induced traps to the quantum wells.	8
6. A few optical absorbance spectra measured at 77K of intersubband transitions in GaAs/AlGaAs MQW samples cut from wafer "A". The samples received different proton doses.	12
7. A few optical absorbance spectra measured at 77K of intersubband Transitions in GaAs/(AlGaAs-GaAs) MQW samples cut from wafer "B". The samples received different proton irradiation doses. The barrier (AlGaAs-GaAs) is a 5 period superlattice.	12
8. Two spectra of intersubband transition in a GaAs/(AlGaAs-GaAs) measured at 77K and 300K for a sample cut from wafer "B" and irradiated with a dose of $3 \times 10^{13} \text{ cm}^{-2}$. Spectrum (b) is the same as spectrum (f) in Fig. 7.	13

9. Total integrated area of the intersubband transitions measured for samples cut from wafers "A" (open squares) and "B" (closed squares) as a function of proton irradiation dose. The solid lines are the results of theoretical fitting. 14

LIST OF TABLES

Table		Page
1.	Structures of the wafers used in the present study. All wafers were Si-doped in the GaAs well to $2.0 \times 10^{18} \text{ cm}^{-3}$. The barrier materials of wafer "B" is made of AlGaAs/GaAs superlattice.	11

1. Neutron Irradiation Effects in $\text{In}_{0.07}\text{Ga}_{0.93}\text{As}/\text{Al}_{0.4}\text{Ga}_{0.6}\text{As}$ Multiple Quantum Wells

Irradiation-induced defects in bulk III-V semiconductors have been the subject of many research interests in the last three decades or so. However, the irradiation effect on interfaces in superlattices and heterojunctions and on various transitions, such as intersubband and interband transitions, in multiple quantum wells have received little attention thus far. Gamma-ray irradiation effect on the intersubband transitions in $\text{InGaAs}/\text{AlGaAs}$ multiple quantum wells have been recently reported. A recent report on the proton irradiation effect on GaAs quantum well lasers indicates that there is a wavelength shift in the lasing spectra.

The interest in irradiation effects on multiple quantum wells and superlattices spurs from the fact that many devices based on III-V semiconductor quantum wells and superlattices are components in systems used for space applications. For example, focal plane arrays fabricated from GaAs related multiple quantum wells for long wavelength application is a sensor used in space for various applications. The prolonged operation of such devices in space environment may results in degradation due to electron, proton, neutron and gamma ray radiation. Thus, it is desired to study multiple quantum well structures that form the basis of long wavelength infrared detectors, under the influence of various radiation effects.

In this section, we present photoluminescence (PL) measurements of interband transitions in $\text{InGaAs}/\text{AlGaAs}$ multiple quantum wells before and after fast neutron irradiation. We will provide possible explanations to the degradation of interband transition as the irradiation dose is increased. The degradation of the interband transition was judged from the dramatic reduction of the normalized integrated area as well as the shift in the peak position energy of the PL spectra.

The multiple quantum well (MQW) structure used in the present study was grown by the molecular-beam epitaxy technique on a semi-insulating GaAs substrate. The wafer consists of 50 periods of 75Å thick $\text{In}_{0.07}\text{Ga}_{0.93}\text{As}$ well and 100Å thick $\text{Al}_{0.4}\text{Ga}_{0.6}\text{As}$ barrier. The well regions were Si-doped $\{[\text{Si}] = 2 \times 10^{18} \text{ cm}^{-3}\}$. The uniformity of the wafer was determined from the peak position of the intersubband transition measurements to be within less than 0.5 meV in samples cut from the center and edge of the wafer. Several samples were cut and irradiated with different doses of fast neutrons beam. An unirradiated sample cut from the same wafer was used in a previous study. The photoluminescence measurements were performed after cooling the sample to a temperature (T) of 25K using a conventional set-up.

It was determined that the MQW structure used in the present study possesses three confined energy levels (E_1 , E_2 , and E_3) in the quantum wells. Based on the doping level in the quantum well regions, it was also determined that the Fermi energy level is located above E_1 and well below E_2 . Thus, one intersubband transition between the ground and first excited states (E_{12} , i.e. E_1 to E_2) should be observed in the optical absorption spectrum of the reference sample. Indeed, this transition was observed and reported. On the other hand, the

PL spectrum originated from the electrons as they decay from E_1 to the heavy hole ground state (HH_1) after the laser excited them. The result is shown in Fig. 1 [see spectrum (a)]. This spectrum appears to be composed of two peaks: one is related to E_1 to HH_1 transition (the peak at around 1.5 eV) and the other transition (the peak around 1.488 eV) is possibly related to the conventional band edge transition in the GaAs substrate.

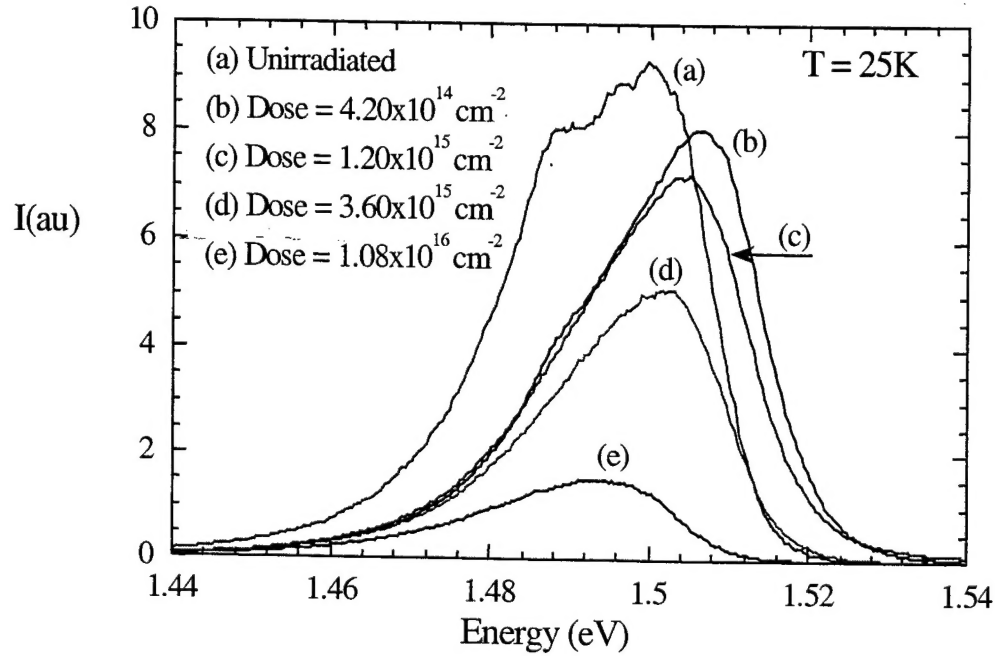


Fig. 1. Photoluminescence spectra obtained at $T = 25\text{K}$ and plotted as a function of fast neutron irradiation dose. Spectrum (a) was obtained for the reference sample (unirradiated). The rest of the spectra were obtained for samples irradiated with different doses as indicated.

Spectra (b), (c), (d), and (e) in Fig. 1 were obtained for samples irradiated with fast neutrons at four different doses of $4.20 \times 10^{14} \text{ cm}^{-2}$, $1.20 \times 10^{15} \text{ cm}^{-2}$, $3.60 \times 10^{15} \text{ cm}^{-2}$, and $1.08 \times 10^{16} \text{ cm}^{-2}$, respectively. It is clear from this figure that the peak at 1.488 eV, which is presumably related to the band edge of the GaAs substrate, almost disappeared in the spectra of the irradiated samples. Additionally, the intensity of the PL peak related to the E_1 to HH_1 transition is dramatically reduced. The normalized total integrated area (I/I_0) of the PL spectra in Fig. 1 is plotted as a function of the irradiation dose and shown in Fig. 2, where I is the total integrated area obtained for the PL spectra of the irradiated samples and I_0 is the total integrated area of the PL spectrum of the unirradiated sample.

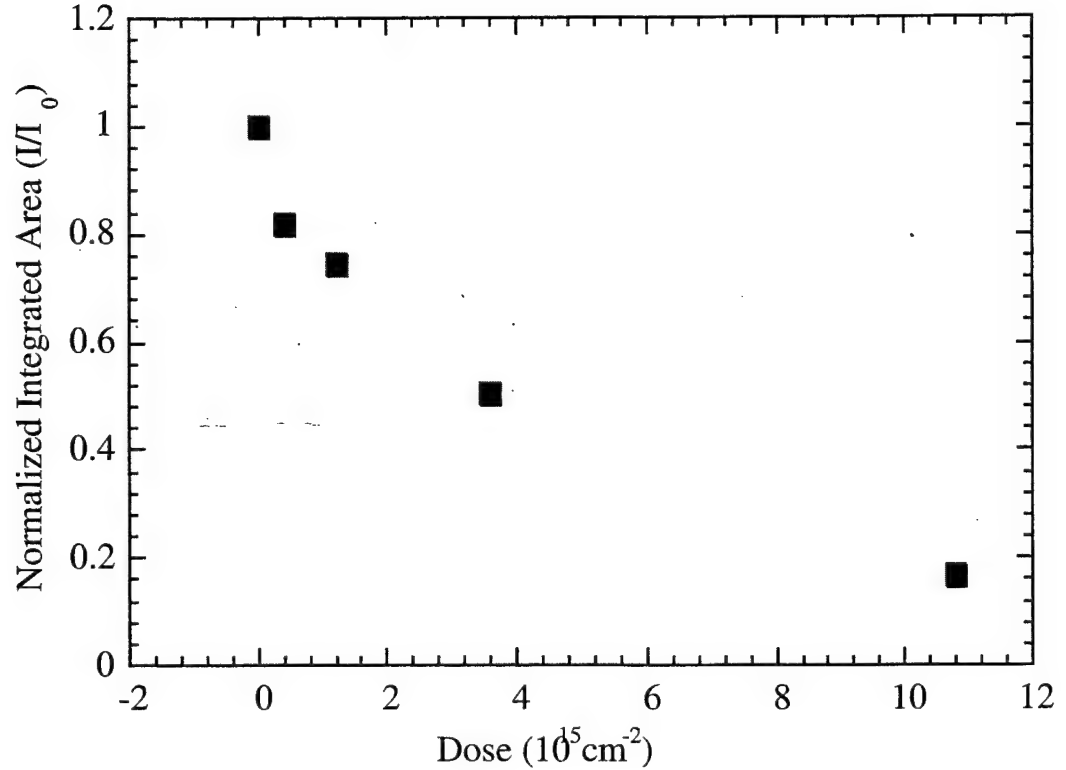


Fig. 2. Normalized integrated area (I/I_0) of the PL spectra plotted as a function of the fast neutron irradiation dose. I_0 is the integrated area of spectrum (a) and I is the integrated area for spectra (b) - (e) in Fig. 1.

The normalized integrated area seems to decrease exponentially as the irradiation dose is increased. The reduction of I/I_0 reflects the decrease of the number of electrons that undergo the interband transition. It is also an indication that the density of states in the conduction band of the quantum well is reduced due to the irradiation-induced damage at the interfaces. The reduction of the density of states limits the number of electrons excited by the laser to jump from the valence band to the conduction band, leading to a significant loss of the PL intensity.

It is noted that the peak position energy of the PL spectra is affected as the irradiation dose is increased as shown in Fig. 3. At first, the peak position energy increased from 1.499 eV for the unirradiated sample to 1.506 eV for the sample irradiated with a dose of $4.2 \times 10^{14} \text{ cm}^{-2}$. Then the peak position energy starts to decrease as the irradiation dose is increased. This behavior could be explained as follows. It is well known that many body effects, in particular exchange interaction and depolarization effect, play a major role in the shifting of the quantized energy levels in the multiple quantum wells. It was determined that the ground

state in the quantum well conduction band decreased as the electron density is increased. It was also observed that the peak position energy of the PL spectrum of the E_1 to HH_1 transition decreased approximately linearly as the doping level is increased in p-type Be doped GaAs/AlGaAs multiple quantum wells. In addition, fast neutron irradiation tends to bring the Fermi energy level toward the center of the band gap, due to the fact the many irradiation-induced point defects such as antisites and vacancies act as electron traps.

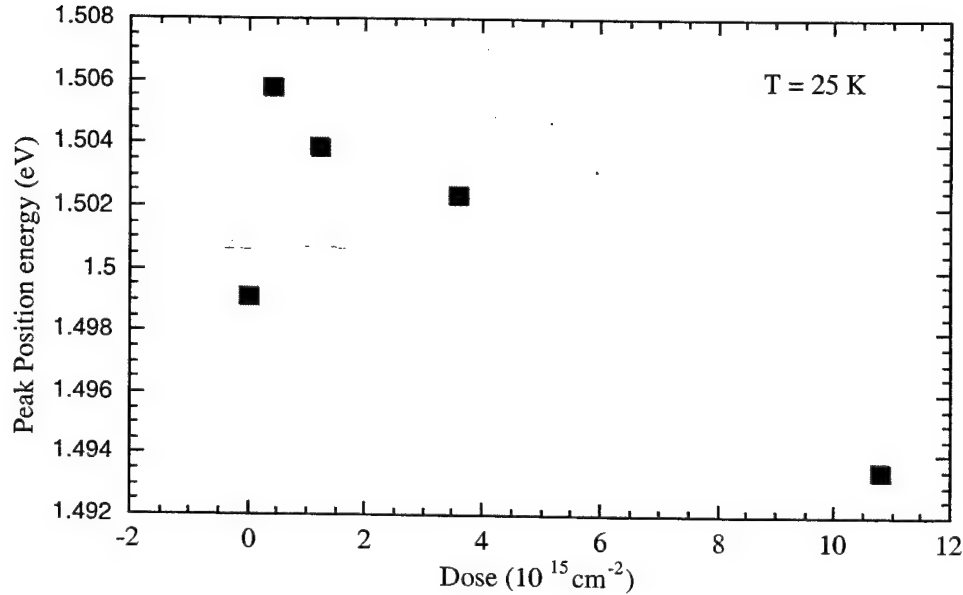


Fig. 3. The peak position energy of the spectra reported in Fig. 1 plotted as a function of the fast neutron irradiation dose.

This leads to reduction of the two-dimensional electron gas density in the conduction band quantum wells. Hence, the ground state (E_1) in the conduction band shifted toward a higher energy. Accordingly, the separation between E_1 and HH_1 increased, leading to an increase in the peak position energy of the PL spectra as illustrated in Figs. 1 and 3.

After the initial increase of the peak position energy of the PL spectrum of the irradiated sample (dose = $4.20 \times 10^{14} \text{ cm}^{-2}$) as shown in Fig. 3, the peak position energy starts to decrease as the irradiation dose is increased. It is even noted that the peak position energy of sample irradiated with a dose of $1.08 \times 10^{16} \text{ cm}^{-2}$ is lower than that of the unirradiated sample (reference sample). It is more difficult to explain this behavior. However, one possible explanation is that the high dose of fast neutron irradiation produces extensive damage at the InGaAs well and AlGaAs barrier interfaces. As a result the ground states (E_1 and HH_1) in both the conduction and valence band quantum wells are brought closer toward the bulk conduction and valence bands maxima of the quantum well material. This leads to a significant red shift of the PL peak position energy.

2. Electron Irradiation Effects in InGaAs/AlGaAs Multiple Quantum Wells

Intersubband transitions in III-V semiconductor multiple quantum wells have been the subject of many studies due to the fact that they form the basis of a new generation of long and very long wavelength infrared detectors. Space application is one of the most recent uses of this class of detectors. For this type of application, it is desired to study the intersubband transitions under the influence of various irradiation effects to determine their survivability and radiation hardness in a space environment. Irradiation effects on the intersubband transitions in GaAs/AlGaAs multiple quantum wells and related compounds have received little attention. Gamma-ray irradiation effect on the intersubband transitions in InGaAs/AlGaAs multiple quantum wells have been reported. Proton irradiation on GaAs quantum well produces a wavelength shift in the lasing spectra. However, the electron, proton, and neutron irradiation effects on the intersubband transitions have not been reported yet. Here we report the electron irradiation effect on the intersubband transitions in n-type $\text{In}_{0.07}\text{Ga}_{0.93}\text{As}/\text{Al}_{0.4}\text{Ga}_{0.6}\text{As}$ multiple quantum wells. It is shown that the intensity of the intersubband transitions is dramatically decreased in heavily irradiated samples, which can be explained in terms of trapping of the two-dimensional electrons by the irradiation induced defects. A negative persistent effect was also observed in the heavily irradiated samples. It is noted that the recovery of the electrons from this effect occurs at two temperature stages with thresholds at $\sim 140\text{K}$ and $\sim 250\text{K}$, which indicates that the electrons were released from two different traps as the temperature is increased.

The multiple quantum well (MQW) structure used in the present study was grown by the molecular-beam epitaxy technique on a semi-insulating GaAs substrate. The wafer consists of 50 periods of 117 \AA thick $\text{In}_{0.07}\text{Ga}_{0.93}\text{As}$ well and 100 \AA thick $\text{Al}_{0.4}\text{Ga}_{0.6}\text{As}$ barrier. The well regions were Si-doped $\{[\text{Si}] = 2 \times 10^{18}\text{ cm}^{-3}\}$. Several samples were cut and irradiated with different doses of either 2 MeV or 5 MeV electrons beams. An unirradiated sample cut from the same wafer was used in a previous study. The infrared absorption spectra were recorded at the Brewster's angle of GaAs (73°) from the normal using a BOMEM Fourier-transform interferometer in conjunction with a continuous flow cryostat. The temperature was controlled within $\pm 1.0\text{K}$.

The MQW structure used in the present study possesses three confined energy levels (E_1 , E_2 , and E_3) in the quantum wells. Based on the doping level in the quantum well regions, it is determined that the Fermi energy level is slightly above the first excited state (E_2). Thus, two intersubband transitions between the ground and first excited states ($E_{12} \equiv E_1$ to E_2) and between the first and second excited states ($E_{23} \equiv E_2$ to E_3) should be observed in the optical absorption spectrum of the reference sample (unirradiated). Indeed, we observed these two transitions in spectrum (a) as shown in Fig. 4. This spectrum was obtained at room temperature and it exhibits two peaks at $\sim 780\text{ cm}^{-1}$ and $\sim 980\text{ cm}^{-1}$, which are assigned to E_{12} and E_{23} transitions, respectively. Spectrum (b) in Fig. 4 was obtained for the reference sample at $T = 77\text{K}$. The peak position energies of both transitions shifted towards higher energies as the temperature is decreased. It is also observed that the intensity of E_{12} transition increased while the intensity of the E_{23} transition decreased as the temperature is decreased.

This behavior can be easily explained in terms of phase blocking and the dropping of the Fermi energy levels as the temperature is reduced from room temperature to 77K.

Spectrum (c) in Fig. 4 was obtained for a sample cut from the same wafer and irradiated with 2 MeV electrons beam. The irradiation dose was $5 \times 10^{17} \text{ cm}^{-2}$. This spectrum exhibits only one transition related to E_{12} . The intensity of this transition is much smaller than that of the reference sample. The E_{23} transition was not observed in the irradiated sample. Similar behaviors were observed in other samples irradiated with the same electron beam but with irradiation doses ranging from $(1 - 4) \times 10^{17} \text{ cm}^{-2}$. However, samples irradiated with 5 MeV electrons beam and doses ranging between $2.0 \times 10^{10} \text{ cm}^{-2}$ and $1.0 \times 10^{12} \text{ cm}^{-2}$ show only a slight difference between their spectra and the reference sample's spectrum. Spectrum (d) is the same as spectrum (c), but it was obtained at 77K. The intensity of the E_{12} transition in spectrum (d) is reduced dramatically, but the transition remains observable. Similar results were obtained in samples irradiated with doses of $(1 - 4) \times 10^{17} \text{ cm}^{-2}$.

It is also observed in Fig. 1 that the peak position energy of the E_{12} transition in the irradiated sample experiences a much smaller shift with temperature than the unirradiated sample. This behavior could be explained as follows. The total integrated area of the intersubband transition is reduced in the irradiated sample, which is an indication that the total number of electrons that undergo this transition is reduced by the trapping mechanism due to the presence of irradiation-induced defects. It was also observed previously that the temperature blueshift in the intersubband transition decreased as the electron density in the quantum well is decreased. Thus, the smaller shift with temperature in the irradiated sample as compared to that of the unirradiated sample can be easily explained in terms of the reduction of the electron density, which in turns reduce many-body effects on the peak position of the intersubband transition.

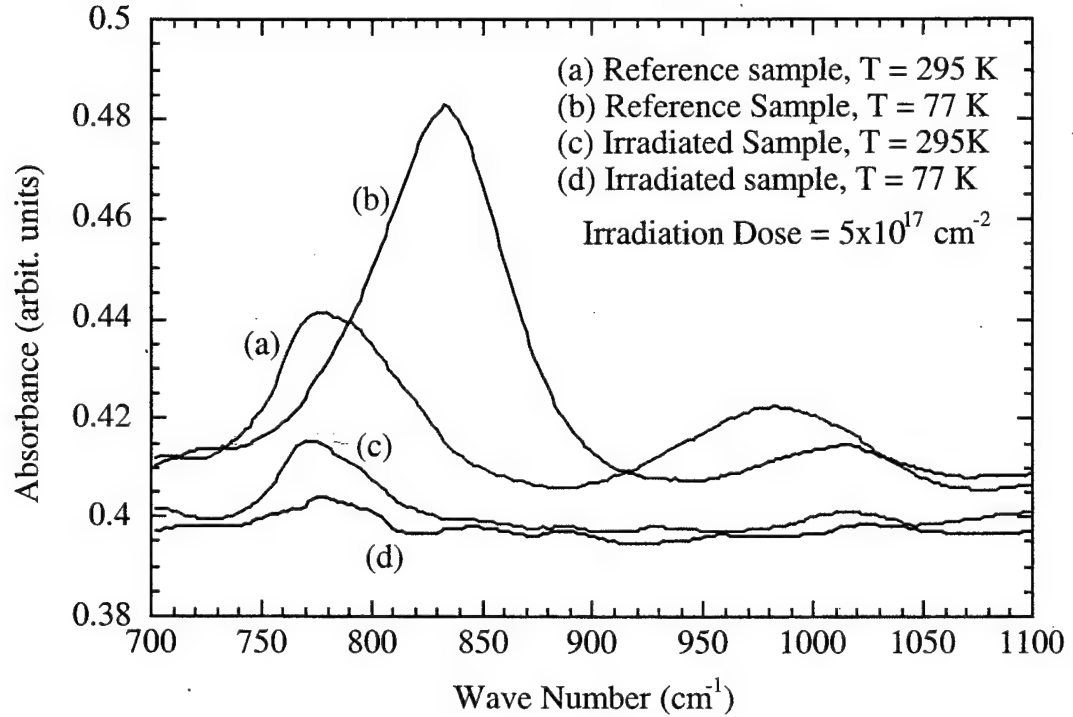


Fig. 4. Optical absorption spectra of intersubband transitions in InGaAs/AlGaAs multiple quantum wells measured at 295K and 77K. Spectra (a) and (b) were obtained for a reference sample (unirradiated) and spectra (c) and (d) were obtained for a sample irradiated with 2 MeV electron beam and a dose of $5 \times 10^{17} \text{ cm}^{-2}$.

The total integrated area of the E_{12} transition in the irradiated sample, which is shown in spectra (c) and (d) in Fig. 4, is studied as a function of temperature. The results are presented in Fig. 5. The total integrated area remains approximately constant between 77K and 140K. A sudden increase in the total integrated area is observed around 150K. A change in the slope of the integrated area as a function of temperature is also observed at around 250K.

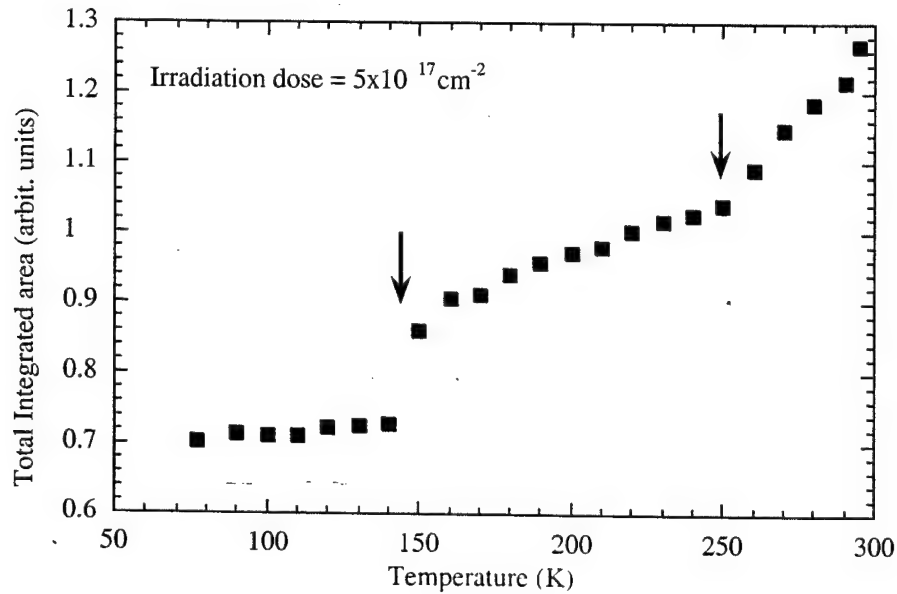


Fig. 5. The total integrated area of the intersubband transition between the ground and first excited states in the electron irradiated InGaAs/AlGaAs multiple quantum wells measured as a function of temperature. The vertical arrows indicate the threshold temperatures at which the electrons are released from the irradiation induced traps to the quantum wells.

It is clear from the present results that the electron irradiation with high doses has drastic effects on the intersubband transitions in InGaAs/AlGaAs multiple quantum wells. Electron irradiation in III-V semiconductors is well known to produce point and complex defects such as antisites, vacancies, interstitials, and various combinations of point defects. In addition, it is anticipated that electron irradiation induced defects may have adverse effects on the interfaces in heterostructures which leads to alternations in the confined energy levels and the two-dimensional electron (hole) gas. Consequently, the interband and intersubband transitions in quantum wells and heterostructures are affected by electron irradiations.

The difference between the intersubband transition spectra, shown in Fig. 4, in samples before and after electron irradiation can be explained as follows. Antisites, interstitials, and vacancies are the primary point defects introduced by electron irradiation. These point defects may form complex defects such as antisite-vacancy, Frenkel pair defects, etc. However, the five primary electron traps in electron irradiated GaAs are E1, E2, E3, E4, and E5. These defects, in particular, E1, E2, and E3 produce energy levels close to the conduction band, which act as electron traps. Thus, by irradiating the InGaAs/AlGaAs MQWs with 2 MeV electrons and doses higher than $1 \times 10^{17} \text{ cm}^{-2}$, one can introduce various defects and electron traps, which can capture electrons from the InGaAs quantum wells. The reduction of the two-dimensional electron gas in the quantum wells can be probed by

measuring the optical absorption of the intersubband transitions. By inspecting the spectra in Fig. 4, one can see the following: First, the total integrated area of E_{12} transition measured at 77 K is greatly reduced as illustrated in this figure by comparing spectra (b) and (d), which are obtained for the reference and irradiated samples, respectively. Second, the E_{23} transition is not observable in the spectra of the irradiated sample, which indicates that the Fermi energy level dropped well below the first excited state (E_2). However, it should be pointed out that mixing between the quantum well and the barrier might occur in the irradiated sample, which may cause the suppression of the E_{23} transition. This possibility requires further studies. Third, the peak position energy of the E_{12} transition in the reference sample [spectrum (b)] shifted from $\sim 830 \text{ cm}^{-1}$ to $\sim 770 \text{ cm}^{-1}$ in the irradiated sample [spectrum (d)]. This red shift indicates that many-body effects, which depend strongly on the two-dimensional electron gas density, decreased among electrons in the quantum well. The above three points strongly suggest that the electrons in the quantum wells are removed from the well through trapping and capturing by irradiation induced defects.

The total integrated area (I) of the E_{12} transition in the irradiated sample [see spectrum (c) in Fig. 1] was tracked as a function temperature as shown in Fig. 5. It is well known that I is directly proportional to the two-dimensional electron gas density. Thus, the measurement of the total integrated area provides a direct monitoring of the total number of electrons that undergo intersubband transitions.

The partial recovery of I around 150K in Fig. 5 is similar to the recovery of the two-dimensional electron gas in the negative persistent photoeffects observed in heavily doped n-type GaAs/AlGaAs multiple quantum wells, which is opposite to the positive persistent photoeffect usually associated with the DX center. However, the effect observed around 150 K in Fig. 5 is not a photoeffect. We may define it as a negative persistent temperature effect, since a secondary light illumination was not used in the present study and the intensity of the global light source in the interferometer was too weak to cause any persistent photoeffects. The fact that we observe a partial recovery around 150K in Fig. 5 is an indication that the electrons may have been released from a Si-related complex defect.

The change in the slope of the data around 250K as shown in Fig. 5, suggests that another shallow defects is involved in capturing the electrons as the temperature is decreased and then releasing them as the temperature is increased. It is difficult to identify the atomic structure of this trap, but it may be related to an arsenic vacancy. This speculation is based on the theoretical calculations of the electronic energy levels of the arsenic vacancy and the arsenic vacancy-gallium antisite pair defects. In conclusion, we have presented new results on the behavior of the intersubband transitions in InGaAs/AlGaAs multiple quantum wells under the influence of 2 MeV electrons irradiation. It is observed that the total integrated area of the intersubband transitions are dramatically decreased after irradiating the samples with doses higher than $1 \times 10^{17} \text{ cm}^{-2}$. This reduction was interpreted as being due to the trapping of the two-dimensional electron gas by the irradiation induced-defects. The total integrated area of the intersubband transition between the ground and first excited state was studied as a function of temperature. The results revealed that two irradiation-induced traps are involved in capturing the electrons as the temperature is lowered to 77K. The electrons

are then released from the traps as the temperature is increased to 300K in two stages with thresholds around 140K and 250K.

3. Proton Irradiation Effects in GaAs/AlGaAs Multiple Quantum Wells

Proton irradiation effect on the intersubband transitions in III-V semiconductor quantum wells has received little attention thus far. The desire to study this effect is based on two factors. First, intersubband transitions form the basis of a new generation of long and very long wavelength infrared detectors. Second, space application is one of the most recent uses of this class of detectors, hence the survivability of these detectors in space and radiation environment becomes very important. Charge ionization and atomic displacement are the most important effects in irradiated semiconductor materials and devices. Charge ionization plays a major role in the device performance since irradiation induced charge-accumulation has a detrimental effect on electronic and optoelectronic devices. Generally speaking, the charge ionization effect is sensitive to the temperature (T_i) at which the irradiation is performed. On the other hand, irradiation induced atomic displacement affects both devices and materials. It is more profound at high doses and less sensitive to T_i .

Irradiation effects on the intersubband transitions in GaAs/AlGaAs multiple quantum wells (MQWs) and related compounds have not been thoroughly studied. Gamma-ray irradiation effect on the intersubband transitions in InGaAs/AlGaAs multiple quantum wells have been reported. Preliminary results on the electron irradiation effects on intersubband transitions in InGaAs/AlGaAs MQWs have been reported recently. A recent report on the proton irradiation effect on GaAs quantum well lasers indicates that there is a wavelength shift in the lasing spectra. However, the proton irradiation effects on the intersubband transitions have not been reported yet. Here we report on the proton irradiation effect on optical absorption spectra of the intersubband transitions in n-type GaAs/AlGaAs MQWs. It is shown that the intensity of the intersubband transitions is dramatically decreased as a function of irradiation dose, which can be explained in terms of trapping of the two-dimensional electrons in the quantum wells by the irradiation induced defects. In addition, we observed that intersubband transitions in samples with superlattice barriers degrade faster than those transitions in samples with bulk barriers as the irradiation dose is increased.

Two multiple quantum well structures used in the present study were grown by the molecular-beam epitaxy technique on a semi-insulating GaAs substrate with 0.5 μm thick GaAs buffer layer and ~ 200 Å thick GaAs cap layer. The structures of the two wafers are shown in Table I. The barriers of the wafer labeled "B" are made of 5 periods AlGaAs/GaAs superlattices, while the barrier of the wafer labeled "A" is bulk AlGaAs. The word "*bulk*" is used here to indicate that the barrier is not a superlattice. The well regions were Si-doped to $2 \times 10^{18} \text{ cm}^{-3}$.

Several samples were cut and irradiated with different doses of 1 MeV proton beam. The infrared absorption spectra were recorded at the Brewster's angle of GaAs (73°) from the normal using a BOMEM Fourier-transform interferometer in conjunction with a continuous

flow cryostat. The temperature was controlled within ± 1.0 K and the spectra were measured at either 77K or 300K.

Table I: Structures of the wafers used in the present study. All wafers were Si-doped in the GaAs well to $2.0 \times 10^{18} \text{ cm}^{-3}$. The barrier materials of wafer "B" is made of AlGaAs/GaAs superlattice.

Wafer	A	B
Well thickness (\AA)	75	105
Barrier material	$\text{Al}_{0.3}\text{Ga}_{0.7}\text{As}$	$\text{Al}_{0.4}\text{Ga}_{0.6}\text{As-GaAs}$
Barrier Thickness (\AA)	100	105 - 35
Barrier period	----	5
MQWs period	50	50

A few spectra of the intersubband transitions in samples cut from wafer "A" and irradiated with different proton beam doses are shown in Fig. 6. The spectra were measured at 77K. Spectrum (a) is obtained for a sample that received a dose of $2.0 \times 10^{12} \text{ cm}^{-2}$, which is identical to the spectrum of the unirradiated samples. This indicates that the above dose did not produce significant atomic displacement damage to cause any change in the spectrum. As the dose is increased, the intensity of the spectra is reduced. However, the intersubband transitions remain observable in samples irradiated with doses as high as $5.0 \times 10^{14} \text{ cm}^{-2}$. The peak position energy of the spectra in this figure is shifted. It was determined by measuring the spectra of the samples before and after irradiation that this shift is due to the non-uniformity of the wafer. It was found that the peak position energies in samples cut near the rim of the wafer are higher than those in samples cut from the center of the wafer.

In Fig. 7, we plotted a few spectra, measured at 77K, of intersubband transitions in samples cut from wafer "B" and irradiated with different doses. By inspecting this figure, we note that a dose of $1.0 \times 10^{12} \text{ cm}^{-2}$ causes some change in the total integrated area as compared the control (unirradiated) sample. We also observed that samples cut from wafer "B" and irradiated with doses higher than $3.0 \times 10^{13} \text{ cm}^{-2}$, do not exhibit intersubband transitions. Spectrum (f) in this figure was obtained for a sample irradiated with $3.0 \times 10^{13} \text{ cm}^{-2}$. The intersubband transition in this sample is still observable. However, upon increasing the sample's temperature from 77K to 300K, we observed two peaks in the spectrum. The results are shown in Fig. 8 where two peaks are observed in the spectrum measured at room temperature.

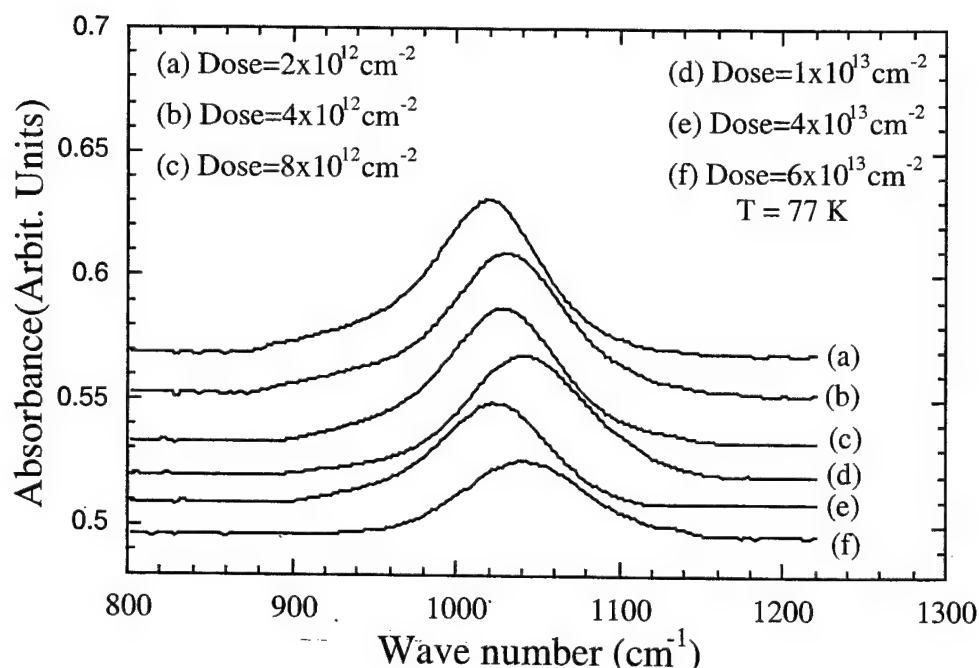


Fig. 6. A few optical absorbance spectra measured at 77K of intersubband transitions in GaAs/AlGaAs MQW samples cut from wafer "A". The samples received different proton doses.

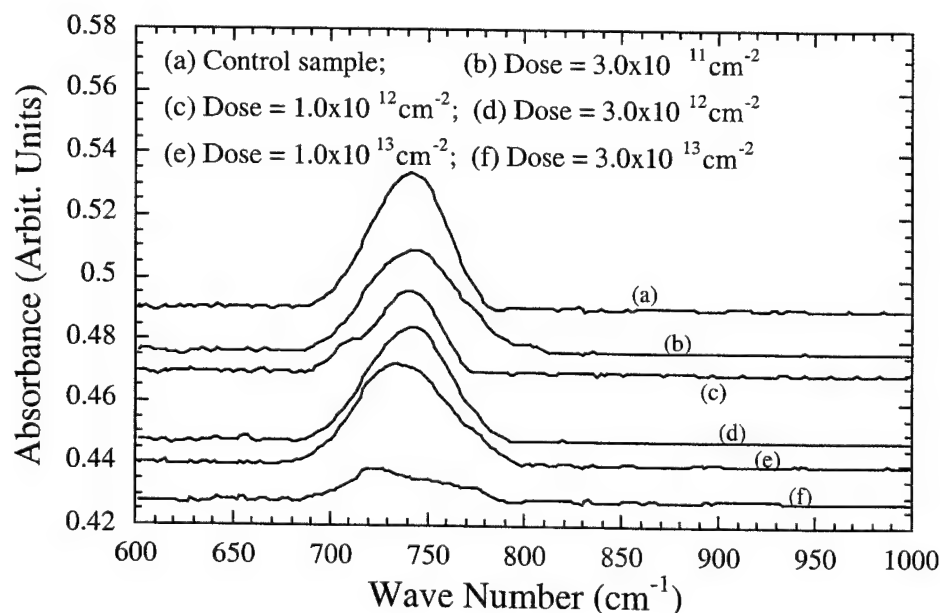


Fig.7. A few optical absorbance spectra measured at 77K of intersubband transitions in GaAs/(AlGaAs-GaAs) MQW samples cut from wafer "B". The samples received different proton irradiation doses. The barrier (AlGaAs-GaAs) is a 5 period superlattice.

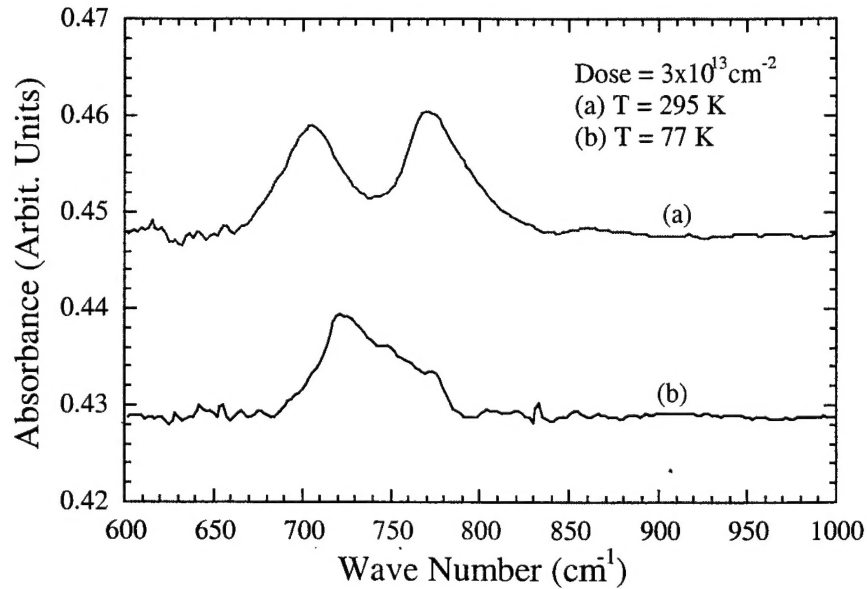


Fig. 8. Two spectra of intersubband transition in a GaAs/(AlGaAs-GaAs) measured at 77K and 300K for a sample cut from wafer "B" and irradiated with a dose of $3 \times 10^{13} \text{ cm}^{-2}$. Spectrum (b) is the same as spectrum (f) in Fig. 7.

The results in this figure could be explained as follows. The structure of wafer "B" was designed such that two bound electronic energy levels (ground and excited states) exist in the well. The excited state is resonant in the miniband that is formed due the superlattice barrier. This miniband consists of five close energy levels. Proton irradiation causes atomic displacement. With a proton beam dose of $3.0 \times 10^{14} \text{ cm}^{-2}$, the damage is significant enough to alter the interfaces so that the energy levels and the miniband in the quantum well structures are shifted. Hence, the excited state in the quantum well is no longer resonant in the miniband. The two peaks in Fig. 8 (a) are thus due to electronic transitions from the ground state in the quantum wells to the first excited state and to the miniband. This plausible explanation is supported by two reasons. First, the two peaks in Fig. 8 (a) were not observed in heavily irradiated samples cut from wafer "A", which does not contain a miniband in its structure. Second, as the temperature is lowered from 300K to 77K, the separation between the two peaks decreases. This indicates that the separation between the excited state and the miniband decreases as the temperature is decreased. Similar behavior is observed in unirradiated samples designed such that the excited state is not resonant in the miniband.

Another interesting observation is seen in Fig. 8. It is noted that the total integrated area of the two peaks in spectrum (a) is decreased as the temperature is lowered from room temperature to 77K. Similar behavior is observed in heavily electron irradiated samples. This effect is designated as a negative persistent temperature effect. It was explained as being due to the presence of irradiation induced defects. These defects trap some of the electrons in the quantum wells (two-dimensional electron gas) as the temperature is lowered. But when the temperature is increased, the electrons are released back to the quantum wells.

The total integrated areas, measured at 77K, of the intersubband transitions spectra were studied as a function of proton irradiation dose. The results are shown in Fig. 9.

The open squares in this figure represent the total integrated area obtained for irradiated samples that were cut from wafer “A”. Integrated areas of the irradiated samples cut from wafer “B” are presented by the solid squares.

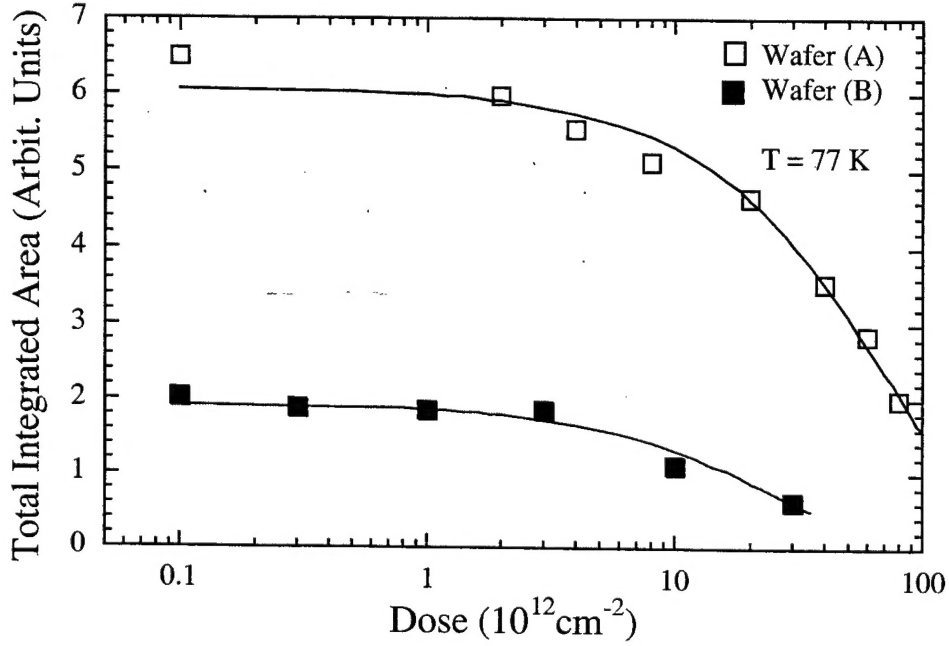


Fig. 9. Total integrated area of the intersubband transitions measured for samples cut from wafers “A” (open squares) and “B” (closed squares) as a function proton irradiation dose. The solid lines are the results of theoretical fitting .

The data in this figure were fitted with the expression $I = I_0 \text{Exp}(-\delta d)$, where I is the total integrated area, I_0 is a fitting parameter but its value is close to the total integrated area of the unirradiated samples, δ is a second fitting parameter, and d is the irradiation dose. The fitting results are shown as solid lines in Fig. 9 for both samples cut from wafers “A” and “B”.

The δ values obtained from the fitting procedure are 0.014 and 0.038 for the samples cut from wafers “A” and “B”, respectively. These values indicate that the samples with superlattice barriers degrade at a faster rate as compared to samples with bulk barrier as the irradiation dose is increased. The above difference in the δ values can be explained as follows. The structure of wafer “B” contains AlGaAs/GaAs superlattice barriers, which means that the number of interfaces is much larger as compared to the structure of Wafer “A”. The proton irradiation produces atomic displacement damage including point and complex defects such as antisites, interstitials and vacancies. These defects play a major role on the quality of interfaces between the epitaxial layers. Hence, samples with smaller

number of interfaces can withstand higher proton irradiation doses as shown for samples cut from Wafer "A". The high δ value in samples with superlattice barriers was also confirmed in another set of MQW samples cut from a wafer with a structure of 59 Å GaAs well and a barrier of 5 periods 59 Å $\text{Al}_{0.4}\text{Ga}_{0.6}\text{As}$ /29 Å GaAs.

4. Conclusions

In conclusion, we reported on photoluminescence measurements for the interband transition in fast neutron irradiated $\text{In}_{0.07}\text{Ga}_{0.93}\text{As}/\text{Al}_{0.4}\text{Ga}_{0.6}\text{As}$ multiple quantum well samples. The PL spectra exhibit a significant degradation in heavily irradiated samples. The peak position energy of the PL spectra was observed to increase and then decrease as the irradiation dose is increased. The reduction of the normalized integrated area and the behavior of the peak position energy of the PL spectra as a function of the irradiation dose were interpreted as being due to the introduction of the irradiation-induced defects in the quantum well and barrier regions as well as due to the damage introduced at the well/barrier interfaces.

We also presented new results on the behavior of the optical absorption spectra of the intersubband transitions in GaAs/AlGaAs multiple quantum wells under the influence of 1 MeV proton irradiation and doses ranging between 1.0×10^{12} and $5.0 \times 10^{14} \text{ cm}^{-2}$. It is observed that the total integrated area of the intersubband transitions is dramatically decreased as the irradiation dose is increased. This reduction was interpreted as being due to the trapping of the two-dimensional electron gas by the irradiation induced-defects. The total integrated areas of the intersubband transitions were studied as a function of irradiation doses for samples cut from wafers with structures containing either bulk or superlattice barriers. The results reveal that the intersubband transitions in samples with superlattice barriers degrade at a faster rate as compared to those transitions in samples with bulk barriers.

DISTRIBUTION LIST

DTIC/OCP

8725 John J. Kingman Rd, Suite 0944
Ft Belvoir, VA 22060-6218

1 cy

AFRL/VSIL

Kirtland AFB, NM 87117-5776

2 cys

AFRL/VSIIH

Kirtland AFB, NM 87117-5776

1 cy

Official Record Copy

AFRL/VSSS/Nathan

Kirtland AFB, NM 87117-5776

2 cys

AFRL/VSS (Dr Polidan)

Kirtland AFB, NM 87117-5776

1 cy